RC23706 (W0508-130) August 23, 2005
Materials Science

IBM Research Report

Localized Electroluminescence of Single-Wall Carbon Nanotubes

M. Freitag[1], J. C. Tsang[1], J. Kirtley[1], A. Carlsen[1], J. Chen[1], A. Troeman[2], H. Hilgenkamp[2], Ph. Avouris[1]

[1]IBM Research Division
Thomas J. Watson Research Center
P.O. Box 218
Yorktown Heights, NY 10598

[2]Low Temperature Division and MESA Research Institute
University of Twente
Enschede, The Netherlands

Research Division
Almaden - Austin - Beijing - Haifa - India - T. J. Watson - Tokyo - Zurich

LOCALIZED ELECTROLUMINESCENCE OF SINGLE-WALL CARBON NANOTUBES

M. Freitag,[1] J. C. Tsang,[1] J. Kirtley,[1] A. Carlson,[1] J. Chen,[1] A. Troeman,[2] H. Hilgenkamp,[2] and Ph. Avouris[1*]

[1] IBM T.J. Watson Research Center, 1101 Kitchawan Rd, Yorktown Heights, NY 10598

[2] Low Temperature Division, Faculty of Science and Technology
and MESA$^+$ Research Institute, University of Twente, Enschede, The Netherlands

[*]avouris@us.ibm.com

8/26/2005

ABSTRACT

Carbon nanotube field-effect transistors emit *mobile light emission* in the ambipolar regime. In the presence of heterogeneities in the local environment of the nanotube, *stationary electroluminescence* is also observed in the unipolar regime, where minority carriers must be generated locally. This *stationary, localized luminescence* can be correlated with changes in the transport current and with an altered movement of the *ambipolar light-emitting spot* during gate- and source-drain-voltage sweeps. Hence, the *stationary electroluminescence* is crucial for identifying "environmental defects" in carbon nanotubes and for evaluating their role in electronic transport. We explore spontaneously doped nanotube segments, which lead to local carrier inversion and electroluminescence. In partially polymer-covered nanotubes, light emission originates at the polymer boundaries, which introduce potential steps along the carbon nanotube. The Schottky contacts of the nanotube field-effect transistors produce large local fields, facilitating light emission. Finally in nanotubes with loops, we observe *localized emission* at the base of the loops but do not observe *ambipolar light emission* from the loops. By using scanning SQUID microscopy on these samples, we measure a finite unipolar current flowing around such loops and show that the nanotube-nanotube junctions at the base of the loops pin the *ambipolar emission*.

I - INTRODUCTION

Carbon nanotube field-effect transistors (CNTFETs) emit infrared light when operated as ambipolar devices. [1-3] The electroluminescence is due to band-to-band radiative recombination of electrons and holes injected from opposite contacts. In short carbon nanotubes (length $<<1\mu m$), the electron and hole currents can overlap over the entire length of the nanotube and the luminescence is therefore distributed over the entire nanotube. In long-channel CNTFETs on the other hand, electron-hole recombination can be faster than carrier transit times through the nanotube, and the luminescence is then localized to a micrometer-sized spot along the tube axis where both the electron and hole distributions are large and overlap. [3] Moreover, unlike a conventional light emitting diode, in a CNTFET there is additional capacitive coupling of the carbon nanotube to a third terminal (the gate), which makes it possible to position the light-emitting spot anywhere along the length of the carbon nanotube. [3,4]

The low-energy electronic transport in CNTs is characterized by very long mean-free paths, suggesting that atomic defects and related heterogeneities do not localize carriers. [5,6] However, charge density fluctuations along the length of carbon nanotubes [7,8] and even localized potential steps have been observed or predicted, [9,10] and such states might modify the electroluminescence from carbon nanotubes. It may even be possible that the high fields and voltage discontinuities associated with these perturbations can produce electroluminescence from unipolar carbon nanotube devices. Recent calculations of the carrier distribution functions in carbon nanotubes at electric fields of the order of $1V/\mu m$ show there are substantial densities of very hot carriers with energies above 0.25eV. [11] Since the energy gaps in 2nm diameter CNTs are of the order of 0.5eV, such hot carrier distributions when combined with local voltage drops of the order of 0.25eV can result in the efficient local generation of electron-hole pairs during unipolar operation.

In this paper, we show that different types of naturally-occurring defects in the local environment of a carbon nanotube as well as purposely-introduced inhomogeneities along long CNTFETs do in fact produce *stationary, localized electroluminescence*. [3] The infrared emission from these sites can be as strong as, or even stronger than the intensity from *ambipolar recombination*. *Stationary emission* does not rely on the ambipolar operation of the FET; in fact we find that the light intensity often increases continuously as the unipolar current increases. We can correlate the stationary emission with the electronic characteristics of the CNTFETs, which helps identify the light-generation mechanism. Most importantly, we can use the emission from known defects to understand their effects on the electronic transport properties of the devices.

Light emission excited by unipolar currents from several types of optically-active inhomogeneities is considered in this paper. The inhomogeneities include (i) Local charge traps in the gate oxide of a CNTFET generated by operation of the FET. (ii) The role of the electric fields due to the Schottky barriers. (iii) Contamination of exposed devices that act as dopants. (iv) Partially polymer-covered carbon nanotubes where the polymer-air interface along the nanotube introduces a dipole. (v) Nanotube-nanotube crossings as present in looped carbon nanotubes. The required electron-hole pairs for the *localized emission* due to unipolar currents are generated by hot carrier impact ionization-type processes at these sites.

II - EXPERIMENTAL DETAILS

Experimental measurements of the light emission from CNTFETs were made using the optical and electrical systems of Ref. [2] with the additional feature that many measurements were performed either in vacuum or an N_2 atmosphere and at temperatures as high as 200C. Images of the light emission were obtained at wavelengths between 1.5 and 2.2μm. The samples were grown from Fe catalysts by CVD [12] on oxidized Si wafers with the heavily doped substrate serving as the gate. The gate oxide thickness was either 100nm or 50nm. The source and drain electrodes were formed by evaporating 20nm of Pd on a 0.5nm thin adhesion layer of Ti. During the process of characterizing the CNTs, two types of devices, one with relatively straight tubes connecting the source and drain, and another with loops where the CNT crossed itself in going from source to drain, were identified by scanning electron microscopy. To reduce hysteresis in the FET characteristics due to charge trapping, some devices were covered by a polymethyl methacrylate (PMMA) layer and annealed. [13] Other devices were only covered partly by PMMA to study the effects of the PMMA-air interface on the optical and electronic properties of these devices.

In the course of this work, it became necessary to independently determine the flow of current through a carbon nanotube that contained a loop, where the current could either go though the junction at the base of the loop or, if the junction was highly resistive, go though the body of the loop. We therefore measured the current-generated magnetic flux by scanning a superconducting quantum interference device (SQUID) in direct contact with the sample. [14] The low-T_c niobium tri-layer SQUID was manufactured by HYPRES; a tab defined by optical lithography was patterned into the sensor pickup loop by field ion beam etching. The bonded and PMMA-protected CNTFETs were directly dipped in liquid helium for this measurement. To improve the signal-noise ratio and discriminate against magnetic

impurities that are present in form of Fe catalyst particles, we used AC bias and lock-in detection of the SQUID signal. An effective pickup loop area of 12.1μm^2 was used for SQUID image modeling, as determined from the measurement of single flux quanta in an optimally doped superconducting $YBa_2Cu_3O_{7-\Delta}$ thin film. The effective height of the pickup loop above the surface for the modeling was set at 6 microns, by comparing the predicted resolution of the meanders in the CNTFET with experiment.

III - RESULTS AND DISCUSSION

(i) Emission induced by charge traps in the gate oxide

Our first examples of local electron-hole pair generation and light emission are small p-doped nanotube segments (Fig. 1) that acts as strong perturbations to the transport current during electron conduction, but *not* during hole conduction. Fig. 1A shows a sequence of infrared images taken during a gate-voltage sweep with fixed drain bias at V_d=-30V (top contact). The nanotube, which is depicted in the first frame, is 60μm long, has a diameter of ~2nm, and exhibits only a few gentle bends. It was completely covered by PMMA to reduce the hysteretic effects [13] in the electronic properties of the device. Because of the length of the carbon nanotube and the large voltage drops across the Schottky barriers at the source and drain, the electric fields in the nanotube at V_d=-30V should be below 0.3V/μm, and comparable to the fields commonly present in smaller devices. The *ambipolar light-emission spot*, where electron- and hole- conducting nanotube segments meet, moves from drain toward source and back from source toward drain during the forward and reverse sweeps. [3] The nanotube segment above the *ambipolar spot* is n-type, whereas the segment below the spot is p-type. There are at least 3 additional *stationary spots*, that each appear once the *ambipolar spot* has moved across them and the corresponding nanotube segment becomes n-type. They disappear on the reverse sweep as soon as the *ambipolar spot* passes them a second time and the corresponding nanotube segment switches back to hole conduction. When source and drain contacts are reversed as in Fig. 1B, *stationary spots* appear at identical positions, again solely in the electron-conduction regime (which is now located below the *ambipolar spot*). The top-most hot spot does show up for both electron and hole conduction and will be discussed later.

As we will show below, the local electron-hole generation and recombination under n-type conduction is likely due to trapped electrons in the SiO_2 close to the carbon nanotube that strongly couple to a small nanotube segment and electrostatically dope it p-type. Trapped charges (electrons or holes) are known to be responsible for hysteretic electronic characteristics of CNTFET. [15,16] Even though the

whole device in Fig. 1 is covered with a thermally-annealed PMMA layer to reduce charge trapping at the exposed oxide surface, [13] a strong hysteresis in the I-V_g sets in at a bias above 15V. [17] The minima in I_{sd} during a sweep of V_g through the ambipolar phase of the FET from p to n and back occur at significantly different gate voltages, depending on the direction of the sweep. Also, the *ambipolar emission spot* moves across the sample during the V_g sweep at different rates, depending on the direction of the sweep. At even higher drain voltages as at V_d=-30V in Fig. 1, qualitative changes occur in both the I-V_g characteristic and the luminescence. Figure 1C shows the disappearance of the minimum in I_{sd} which normally appears as the bias is swept from p to n-type in an ambipolar FET. The minimum is still present on the reverse sweep from n to p-type conduction. The observed motion of the *ambipolar emission spot* occurs at smaller values of V_g (V_g~-2V) than expected when extrapolated from low-drain-bias results (V_g~-10V, data not shown). Much more current noise is observed in the n-type or ambipolar regime than in a purely p-type regime (Fig. 1C). Finally, the additional *stationary emission spots* appear along the tube in the n-type conduction regime.

Trapped electrons in the gate insulator can act like an additional negative gate-voltage for the carbon nanotube, which means that more positive voltages at the gate will be needed to produce n-type conduction. Trapping and de-trapping of charges will also lead to noise in the transport current. Moreover, the actual voltage ranges at the drain, source, and gate contacts (-30V, 0V, and -4V to 0V in that order) create favorable conditions for electron injection from the carbon nanotube into the oxide, especially in the vicinity of the drain contact: Considering the field-focusing due to the nanometer-sized radius of the carbon nanotubes we can expect large transverse electric fields in the immediate vicinity of the nanotube surface. [15] Oxide traps below the passivated SiO_2 surface should then be accessible. As the *ambipolar spot* in the carbon nanotube moves from drain toward source, a growing nanotube segment (between the drain contact and the ambipolar region) becomes n-type and therefore a growing oxide region in the nanotube vicinity can become negatively charged. In Fig. 1C on the sweep from -4V to 0V, electron conduction in the vicinity of the drain starts at around -3V, and immediately electrons get trapped close to the drain, which limits an otherwise expected increase in electron current during this sweep all the way to V_g=0V. On the other hand, during the reverse sweep from 0V to -4V, no additional charge trapping happens as the *ambipolar spot* moves back toward the drain, and the current goes through a well-defined minimum. [18] Since the carbon nanotube devices are Schottky barrier transistors, [19] the charge trapping at the metal to nanotube contacts dominate the hysteresis in the IV characteristics.

Even though we can not entirely rule out local doping by impurities or atomic vacancies, the presence of strong trapping of negative charges, in connection with the n-p-n nature of the s*tationary,*

localized luminescence strongly suggests that electron traps are also responsible for the light emission. We will also see in section (iii) that these kinds of junctions can be produced in real time by large gate fields, making it unlikely that the ones observed here pre-exist before applying large voltages. For a p-type carbon nanotube, not much changes upon electrostatic doping by trapped electrons except that the local carrier density might increase slightly. For an n-type nanotube on the other hand, inversion could occur at sites where sufficient charge is trapped close to the carbon nanotube, and n-p-n junctions would then be formed along the CNT, blocking the channel. [20] Band to band light emission could then arise in two different ways (Fig. 1D). In one case, where the blocking region is large, the forward-biased pn junction acts as the light-emitting diode, whereas the backward-biased pn junction is operated in a Zener-tunneling regime (shown in green in Fig. 1D). [21] Without efficient band-to-band tunneling at the backward biased pn junction, the p-type segment would be immediately neutralized upon biasing and the luminescence would cease. It has been shown recently, [22] that this kind of band-to-band tunneling can actually be produced in carbon nanotubes, even with dual-gate technology where the gates are much further removed from the carbon nanotube than a typical trap location. Trapped charges close to the carbon nanotube are expected to produce potential fluctuations on the nanometer length-scale, leading to abrupt pn junctions that should be very efficient for Zener tunneling. In addition, the carbon nanotubes used here have considerably smaller bandgaps than the ones used by Appenzeller et al. [22], increasing the tunneling probability further. Alternatively, (depicted in red in Fig. 1D), the forward-biased pn junction can inject carriers in the base-like p region, and if the base-like region is small so that most of the injected carriers could pass through the p-region, they will be injected into the back-biased pn junction as in the case of a bipolar transistor. [21] If the band offsets for the reversed biased pn junction, and the excess energy associated with hot carrier effects in our carbon nanotubes are together comparable to the bandgap of the carbon nanotube, then electron-hole pairs generated by the hot carriers will produce light emission.

(ii) Role of the electric fields due to the Schottky Barriers.

We now turn to the metal-nanotube contact regions in CNTFETs, where we also often observe *stationary, local electroluminescence* for one type of polarity (either electrons or holes) but not for the other. The large electric fields present at the contacts enhance charge trapping there and make the above discussed n-p-n luminescence mechanism (or an analogous p-n-p mechanism in case holes get trapped) more likely near the contacts. Both contacts to the CNTFET in Fig. 1 behaved like n-p-n junctions during

recorded sweeps prior to the one in Fig. 1B. The top contact showed up exclusively during n-type conduction (e.g. Fig. 1A), as did the bottom contact (e.g. Fig. 1B). The top contact however changed its light-emitting behavior at the end of the sweep in Fig. 1A, where a rapid increase in luminescence intensity of 5X occurred, while the *ambipolar spot* was positioned there.

To explain this behavior, we note that during the reverse sweep in Fig. 1C, as the nanotube becomes more p-type, the character of the light emission near the contact gradually changes from *ambipolar* (due to direct injection of the electrons from the drain) to *unipolar* (due to large local fields that promote impact ionization). In the absence of high-field carrier generation mechanisms, we would expect the *ambipolar emission intensity* at the contact to decrease monotonically with gate voltage, because the minority carrier injection from that contact decreases with the gate voltage. This is what is usually observed when the current is kept constant during $V_d(V_g)$ sweeps. [3] For fixed V_d however, the light emission from the contact with which the *ambipolar spot* merges, never totally ceases. In fact it usually keeps on rising, which means that the potential landscape along the nanotube must shift dramatically. Tersoff et al. [4] have obtained a square root dependence of the carrier number density as a function of the distance from the *ambipolar spot*. The longitudinal electric field is thus highly concentrated at the *ambipolar region*. Upon reaching a contact, the high fields associated with the *ambipolar region* are concentrated in an area, where a discontinuity (the metal-nanotube Schottky contact) already exists. This leads to impact ionization and avalanche carrier multiplication in this region, producing strong luminescence from hot carrier recombination.

In Fig. 1A and 1C, the luminescence from the top contact first increased gradually as described above, but near V_g=-4V it turned up sharply. The transport current during this event was 27μA, an extremely high value at which carbon nanotubes are well known to get irreversibly damaged. Afterwards, the top contact showed luminescence in both n- and p-type conduction regimes. We have seen infrared emission from both polarities of carriers in the contact area in other devices as well. Here we can pin-point the creation of the defect because we have visual snapshots of what happened during the sweep after which the behavior changed.

(iii) Emission induced by surface impurities on exposed CNTFETs

Figure 2 shows a different CNTFET where we found strong *stationary light-emission sites* which could appear while the FET was being operated. This device is not covered by a polymer and the data on this carbon nanotube were taken at an elevated temperature of 200°C because the current minimum where

ambipolar conduction occurs was very low and increasing the temperature increases the transmission through the Schottky barriers for both electrons and holes. It turns out that even at elevated temperatures the *ambipolar spot* moves rapidly from one contact to the other during gate-voltage sweeps, confirming that most of the bias voltage still drops at the contacts. [4] In a dry nitrogen environment, as in Fig. 2A, the *ambipolar spot* flickers between source and drain for a substantial range of gate-voltages. The flickering happens so fast that the shortest camera integration time of 250ms available in our HgCdTe camera was insufficient to resolve the movement of the *ambipolar spot* and the whole nanotube appears to light up at once. Fast charge trapping/de-trapping close to one of the contacts is the likely cause of this erratic luminescence behavior. In air, as in the sequence in Fig. 2B or the projection of the light emission along the tube as a function of time in Fig. 2C, the *ambipolar spot* jumps only once from the bottom to the top contact around a gate voltage of 28V (solid line in Fig. 2C). Additionally, when forced by the voltage on the backgate into strong hole conduction, *stationary spots* appear one-by-one, similar to the n-p-n junctions observed previously in Fig. 1. Here however, the charges trapped close to the carbon nanotube during the gate voltage sweep are holes and an oxide charge induced junction would be of the p-n-p type. No trapping of electrons is observed in the electron-conduction regime, which occurs at the left end of Fig. 2C.

It is not clear what determines the type of carriers being trapped in our devices. Electron traps as observed in Fig. 1 should be generally present in silicon oxides. [23] We note that around the device shown in Fig. 2 we observed process/handling related debris with an optical microscope and it is possible that the hole traps in this unprotected device are associated with these impurities and the moisture in the air rather than the oxide itself. It should also be noted that in subsequent runs some of the spots did not re-appear, while additional ones were formed in real-time, whereas in the clean device in Fig. 1 spots always appeared at identical positions. Correlating the I-V_g curve in Fig. 2C with the simultaneously acquired luminescence movie gives additional information about the light emission mechanism. Each time a new *stationary spot* appears the overall current through the carbon nanotube drops as indicated by the arrows in the figure. This is evidence for a significant redistribution of the potential drop along the device. A new potential step associated with the formation of a defect leads to a decreased potential across the un-disturbed portions of the tube and the current drops. From the current reduction of around 10% and the bias of 40V the associated potential drop at the new p-n-p junction is estimated to be several volts.

The strong effect of single defects on the current in our system is a result of the 1D nature of the conduction through a carbon nanotube. In 3D materials the current can easily avoid a localized defect, while in a true 1D material the current has to go through the defect. One needs to note however that

geometrically, a carbon nanotube is quasi-1D in the sense that it is not a single chain of atoms, but rather a cylinder. Due to its smallness, only one electronic sub-band is usually populated. Its cylindrical shape makes a carbon nanotube less susceptible to atomic-scale defects than, for example, poly-ethylene, because the current can still be carried through the rest of the ring structure even with certain defects in its structure. [6] However, in the presence of stronger scatterers such as the top-most defect in Fig. 1B, or when an entire nanotube ring-segment gets electrostatically inverted by near-by localized charges, as in the case of Figs. 1 and 2, the defects have a strong influence as one would intuitively expect for a true 1D material. [20]

In Figs. 1 and 2, the fluctuations along the tube are randomly generated and distributed. The behavior of the light emission with changing biasing conditions and the well-understood hysteresis in the I-V_g sweeps suggests that trapped charges are responsible for the formation of locally-doped nanotube segments. It would be very desirable to independently determine the nature of a defect or introduce well-defined defects. In Fig. 3 we therefore produced a discontinuity along a 50μm long CNTFET by covering half of the nanotube including one contact with PMMA. The other half is either exposed to air or nitrogen. The nanotube in Fig. 4 has loops that introduce tube-tube crossings acting as well-defined inhomogeneities in the CNTFETs.

(iv) Effects of a dielectric boundary atop a CNTFET

First we consider the nitrogen-PMMA boundary in Fig. 3. An SEM image of the completed device (Fig. 3A) shows the PMMA layer covering the top half of the device including the top contact. The carbon nanotube and the gap between the two contacts are about 50μm long. Figures 3B-E show the projection of the electroluminescence onto a line connecting source and drain during various V_g sweeps in which source and drain contacts, as well as the drain polarity, were permutated as indicated in the figures. During the sweeps, I_{sd} goes through two broad minima, which is the signature of ambipolar conduction. [19] For example in Fig. 3B, the CNTFET is initially n-type (injection of electrons at the top contact), then becomes p-type (injection of holes at the bottom contact), and finally returns to n-type. The transition from one type of conductivity to the other type involves a continuous decrease in the density of the first type of carriers and an increase in the density of the second type of carriers, with the cross over between the two types producing a minimum in the conductivity of the channel. In long-channel CNTFETs, such as the ones used here, the location of the cross-over point between the two types of carriers, which can be

identified by its *moving light emission*, travels across the length of the carbon nanotube as the gate voltage is varied.

In homogeneous devices, the motion of the *moving ambipolar spot* during gate-voltage sweeps is smooth. [3,4] However, anomalous behavior in the *moving spot luminescence* was observed in half-PMMA-covered CNTFETs, as well as other heterogeneous samples. During the sweeps in Figs. 3C and 3D, after the *ambipolar spot* emerges from the nitrogen-exposed region of the CNTFET, it briefly halts at the PMMA boundary for about 3V change in gate voltage, before proceeding in the polymer-covered region. The kink in the motion of the *light-emission spot* is mirrored by structure in $I_{sd}(V_g)$. On the other hand in Figs. 3B and E, the spot moved smoothly across the boundary.

Tersoff et al. [4] showed that the *motion of the light-emission spot* in ambipolar devices can be described by a simple drift-diffusion model. In this model the gate voltage couples capacitively to the carbon nanotube and induces the charges (electrons or holes) in the tube that carry the transport current. The *ambipolar light-emission spot* lies at the overlapping segment between the electron and hole regions in the CNT where there is no net charge. As a result, the tube potential at this spot is approximately V_g. As V_g changes between the source and drain voltages, the *ambipolar emission spot* moves between source and drain. For a homogeneous tube the movement of the *ambipolar spot* is smooth and continuous, because the voltage drop along the device is smooth. Inhomogeneities, such as the PMMA boundary, will modify the motion of the *ambipolar spot* if they are associated with additional local voltage drops. This is what we see in Figs. 3C, D and many other instances of purposely-introduced or random defects. Within this model, a local potential drop can be quantified by the additional gate voltage that is needed to move the *ambipolar spot* across the inhomogeneity. We can therefore estimate the PMMA-boundary-related potential drop to be about 3V under the biasing conditions in Figs. 3C and 3D. The 3V may drop over a region as large as a few μm, the lateral resolution of our optical setup, but it is likely to be much more localized than that.

In the half-PMMA-covered CNTFET, a dipole should arise from the different effective dielectric constants in the PMMA-covered and un-covered regions. The higher effective dielectric constant in the polymer-covered region increases the capacitive coupling between nanotube and gate, which leads to larger induced charge densities in the nanotube in the polymer-covered region. However, when the *ambipolar spot* passes by the PMMA boundary, the boundary is on the gate potential and no charges are induced there. [4] The gate-induced dipole could therefore be important in the unipolar regime, but not in the ambipolar regime as required here.

Another dipole arises in case of unequal oxide charge trapping at the two sides of the PMMA boundary. The observed slowing down of the *ambipolar spot* at the boundary under some biasing conditions (Figs. 3C and D, negative, exposed drain or positive, protected drain), but not under others (Figs. 3B and E, negative, protected drain or positive, exposed drain) is consistent with an excess of trapped electrons in the exposed region. The resulting dipole points from the PMMA-covered to the N_2-exposed region, as indicated to the left of Fig. 3B. In Figs. 3C and D, the dipole is oriented to increase the local potential drop across the boundary, and the spot slows down. This situation is depicted schematically in Fig. 3F. The horizontal lines indicate different gate voltages, between the source and drain voltages, that are spaced equally. The point where these lines cross the chemical potential in the tube (assumed mid-way between conduction and valence bands as the *ambipolar spot* is positioned there) determines to first order the position of the *moving light-emission spot*. [24] The spot is therefore expected to slow down at the boundary. The intensity of the *ambipolar light emission* at the boundary increases because of the higher fields there. In Figs. 3B and E on the other hand, the dipole is oriented against the externally applied voltage. Under bias, current continuity requires that charges are accumulated in the carbon nanotube to counteract the effect of the opposing dipole until the potential step is smoothed out (Fig 3G). For n-type conduction, electrons accumulate in the PMMA-covered region of the nanotube, for p-type conduction, holes accumulate in the exposed region of the tube, and for ambipolar conduction a combination of the two can accumulate. The boundary then has very little effect on the movement of the *ambipolar spot*.

The speed of the *ambipolar spot* around the boundary in Fig. 3C is also dependent on the direction of the gate-voltage sweep. On the forward sweep, where the *ambipolar spot* moves from the PMMA-protected to the N_2-exposed region of the nanotube, the spot barely stops at the boundary, while on the reverse sweep, where the *ambipolar spot* moves from the exposed to the protected region, we observe the pronounced retardation. This indicates that electron trapping happens predominantly close to the *ambipolar spot*, where the carriers are activated by the high fields there. When the *ambipolar spot* travels from the protected region across the boundary, not much electron trapping has occurred yet. Once the spot has crossed into the exposed region, trapping starts in earnest, which explains the instability (rapid forward-backward movement) of the *ambipolar spot* in this regime. On the reverse sweep, the *ambipolar spot* has already conditioned the oxide and upon receding across the boundary it slows down due to the built-up dipole.

A second CNTFET that was also partially covered by PMMA and the light emission from this device are presented in Figs. 3H-I. An SEM image of the completed device, displaying the PMMA layer

that covers the top half of the device and the drain, is given in Fig. 3H. The data in Fig. 3I corresponds to a gate-voltage sweep from 0V to 30V and back to 0V at V_d=35V. The CNTFET was initially p-type, then became n-type, and finally returned to p-type. The I-V_g curve shows considerable hysteresis, and the I_{sd} minimum for the initial p to n sweep is much larger (5μA) than for the final n to p sweep (1μA), due to preferential trapping of electrons near the (unprotected) source contact. Therefore the *moving spot luminescence* is only resolved on the forward sweep and its behavior, including the retardation at the boundary, is similar to the previously discussed sample under the biasing conditions of Fig. 3D.

Figure 3I was part of a series of successive identical V_g sweeps. Initially the sweeps produced light emission that was qualitatively similar to the pattern shown in Fig. 3D. Starting from the second sweep however, an additional *stationary light-emitting spot* appeared suddenly at the PMMA boundary (Fig. 3I) and disappeared again during the back sweep. The luminescence at the drain becomes much weaker after the PMMA boundary related luminescence appears. The new *light-emission spot at the PMMA boundary* is an order of magnitude more intense than the luminescence at the *moving ambipolar spot*. The onset of *luminescence from the PMMA boundary* is accompanied by a 1μA drop in current, as seen in the I_{sd} trace in Fig. 3I. Conversely, the disappearance of the *PMMA boundary-related luminescence* is associated with an increase in current. These results suggest that the abrupt decrease in I_{sd} marked by the two arrows in Fig. 3I is accompanied by a substantial redistribution of the potential across the nanotube.

The mere presence of electrons in the carbon nanotube, as is the case once the *ambipolar luminescence* passes by the PMMA boundary, is not sufficient to induce the *stationary light emission from the polymer boundary*. Note the analogy to the sample in Fig. 3C, where the presence of electrons in the tube on the forward sweep was not sufficient to produce the dipole across the boundary that slows down the *moving ambipolar spot*. In that case, hot electrons from the *ambipolar spot* were necessary to overcome a barrier for charge trapping in the oxide. In Fig. 3I, the large applied gate fields move the Fermi level well into the nanotube conduction band, which also reduces the tunneling barrier for electron trapping in the gate oxide. At a sample-history-dependent threshold, the gate field is large enough to extract significantly more electrons from the tube than was possible by positioning the *ambipolar spot* there. The resulting dipole produces a localized longitudinal electric field that accelerates the electrons in the carbon nanotube across the boundary, so that impact ionization can produce new electrons and holes, which can recombine and emit light with more than ten-fold increase in luminescence intensity from a given nanotube segment. The magnitude of the oxide charging increases with the total current which passes through the device explaining why the PMMA boundary emission only appears after the FET has

been operated for some time. The development of this dipole would produce a decrease in the potential drops across the Schottky barriers, explaining the decrease in current and the decrease in light emission from the contacts, as the *polymer-boundary light emission* appears.

(v) Electroluminescence at the crossing of a CNT loop

We now turn to carbon nanotubes containing closed loops which we incorporated in CNTFETs. In these devices a single carbon nanotube connects source and drain contacts, but does so by crossing over itself a few times in between (see for example Fig. 4A, 4B, and the inset in Fig. 5B). The current can be carried around the loops or it can flow through the nanotube-nanotube junctions at the crossings, and it is unclear to what extent one or the other should happen. In addition to the unknown current path, the effect of the loops on the movement of the *ambipolar light-emission spot* during gate-voltage sweeps is an open question. The presence of the loops does not appear to have a qualitative effect on the electrical characteristics of the tube. As shown in the overlay in Fig. 4B, the plot of $I_{sd}(V_g)$ at V_d=-40V had a well defined minimum in I_{sd}, characteristic of the ambipolar behavior of the CNTFET.

Figures 4A and 4C show the electroluminescence from a CNTFET with loops, obtained by overlaying the individual frames of infrared movies that were taken during two different gate-voltage sweeps. To identify the position of the three loops in this device, we superimposed an SEM image on both electroluminescence images. The light emission follows the geometry of the carbon nanotube channel, but no light is observed from the three nanotube loops. Enhanced luminescence from the three nanotube-nanotube crossings stems partly from a slower movement of the *ambipolar spot* at these positions, but also from additional *stationary luminescence* at the tube-tube crossings that we will discuss below. Given our signal to noise ratio we estimate that any light emission from the loops is at least 10-20X weaker than the *moving spot emission* from the sections of nanotube connecting the three loops.

Figures 4B and 4D are static representations of the time-resolved light emission from our sample during the different V_g sweeps, where the y axis is the projection of the luminescence on a perpendicular line between the source and the drain, and the x axis corresponds to the time for the $V_g(t)$ sweep. Since the CNT is not straight, different intervals along the y axis do not correspond to the same distance along the CNT. However, the positions of the loop crossings on the CNT have distinct positions on the y axis. Infrared movies of the entire sweeps can be accessed online. [Supporting material] The *moving spot emission* moves smoothly along most of the carbon nanotube except at the loops themselves. At each tube-tube crossing the spot slows down before continuing on the next nanotube segment. Under the

biasing conditions in Fig. 4B, electrons are injected at the bottom contact and holes at the top, while in Fig. 4D the injection is reversed (electrons at the top and holes at the bottom). Between Figs. 4B and 4D, the source and drain biases were reversed, but at the same time the gate voltage sweeps were reversed. This accounts for the similar U-shaped movement of the *ambipolar spot* in Figs. 4B and 4D.

To answer the question of the dominant current path under unipolar biasing conditions, we have measured the magnetic flux generated by the current through looped CNTFETs with Scanning SQUID Microscopy (Fig 5). [14] Figure 5A and 5B show modeled magnetic flux images for a CNTFET with two loops, assuming that all the current flows through the tube-tube junctions (Fig. 5A), and alternatively assuming that all the current flows along the loops (Fig. 5B). An SEM image of the CNTFET is shown as an inset to Figs. 5A and 5B. We wire-bonded the contacts at the far right, which is why the left parts of the leads carry no current and do not show up in the images. The increased magnetic flux at the center of the two loops in model 5B is the result of the additional loop current. Figures 5C and 5D show our experimental result for the magnetic flux generated by this CNTFET at a current of 2μA. Three separate images were added to increase the S/N ratio. A small, gradual reduction in transport current during the sweeps (slow axis from top to bottom) was corrected for in these images. In Fig. 5C the color scale is chosen similar to the one in the models (Fig. 5A and 5B) to facilitate a visual comparison, while in Fig. 5D the whole data range is shown. The full scale variation of flux through the pickup loop was 1.5·10E-4Φ_0, where Φ_0=h/2e is the superconducting quantum of flux. Figure 5E is a line scan across the carbon nanotube (as indicated in Fig. 5D) that shows the field changing sign when the pick-up loop traverses the nanotube. Figure 5F shows a line scan parallel to the carbon nanotube that includes the location of the two loops.

From the visual comparison of the experimental and modeled images as well as from the line scans in Fig. 5F it is apparent that there is enhanced magnetic flux at loop #1. Most of the current is therefore flowing around this loop. The situation at loop #2 is different and more consistent with the model that does not include current going around the loop, which means that most of the current should tunnel through this nanotube-nanotube junction. We estimate that the noise in our data is about 1/2 of the expected signal from the loops, which prevents us from quantifying exactly what the loop/tunneling current ratio is at the two loops. However, the signal at loop #1 is clearly above the noise floor and there must be current around this loop.

Our electroluminescence and SQUID measurements on looped CNTFETs tell us that the boundary between electron and hole currents (the *mobile ambipolar light-emission spot*) does not travel around the nanotube loops the usual way, even though a significant unipolar current can flow around

them. While sweeping the gate voltage, the *ambipolar spot* instead gets pinned at the tube-tube junctions. Our previous work on light emission from ambipolar carbon nanotube FETs demonstrated the dominant role of electron-hole recombination in carrier transport in carbon nanotubes since we found that the spatial overlap between the electrons and holes (recombination length) was at the limit of our instrumental resolution. Our results in Fig. 4 show that electron-hole recombination remains a fast process in our looped tubes at the loop crossings so that only a small fraction of the electrons and holes injected into these nanotubes make it past the loop crossing and into the body of the loop. Excitons (bound electron-hole pairs) have generated a lot of attention in the carbon nanotube field recently, because they are much more strongly bound in this 1D material than in usual 3D bulk materials. [25,26]. Exciton effects involving the long range coulomb interaction between electrons and holes at our loop crossings will still be strong given the confined geometry of the crossing.

In addition to the *moving spot emission*, Figs. 4B and 4F show *stationary luminescence* at the nanotube-nanotube crossings under unipolar bias, reminiscent of the defect-related *stationary luminescence* in Figs. 1-3. The strongest *stationary luminescence* from most of the crossings is observed in the p-type conduction regime (inside the U-shaped region in Fig. 4B and outside of the U in Fig. 4D). In general, the intensity of the light emission from the crossing points increases with increasing unipolar current.

If each loop in Fig. 4A includes about 12% of the total length of the tube, then to first order, about 12% of the voltage drop across the total tube will be across a loop if all the current went through the loop. If only a fraction of the current goes through the loop, then the voltage drop across it will drop proportionately. From Tersoff et al., [4] the voltage drop across the carbon nanotube can be estimated by the magnitude of the swing in V_g required for moving the *ambipolar light-emission spot* from one end of the CNT to the other end. We find that this is about 6V so that we estimate that the voltage drops across the tube-tube crossings at the bases of our nanotube loops must be less than ~700mV. The current through the CNTFET is on the order of 10μA, which gives a resistance for the loop on the order of 70KΩ.

Fuhrer et al., [27] who studied crossed CNTs in two- and four-probe geometries, found experimentally that there was significant transmission between two touching semiconducting nanotubes ($R_{inter\text{-}tube} \leq 400K\Omega$, corresponding to $T \geq 1\%$). They estimated that a tunneling distance set by the van-der-Waals attraction between the tubes (0.34nm) would be insufficient to explain this transmission. When the distance between the crossing nanotubes was reduced to a distance of 0.25 nm, consistent with the expected deformation of the tubes at the junction, [28] the calculated transmission of the crossing was close to what they measured. The CVD-grown nanotubes that we are using here are much larger in

diameter (~2-3nm) than the laser-ablation grown tubes that Fuhrer et al. used (~1.3nm). This should decrease the tunneling resistance by at least a factor of 4 because of the larger contact area between the tubes. Using a value of 100KΩ for the tunneling resistance would mean for us that ~40% of the current is tunneling through the junction, while ~60% goes through the loop, and the voltage drop at the junction is reduced from 700mV to 400mV.

Related results were obtained by Paulson et al. [29] for the carbon nanotube on graphite system. They measured a low contact resistance between a carbon nanotube and graphite substrate and found a strong dependence of the contact resistance on the angular orientation between a carbon nanotube and the graphite lattice. A similar effect has been predicted for tunneling between two carbon nanotubes. [30] The exact angle at which the tube crosses over itself could therefore account for an order of magnitude change in tunneling resistance at the tube crossing. This might explain why loop #1 in Fig. 5 shows a current around the loop, while loop #2 does not. It could also explain the very different electroluminescence intensities measured at the three loops in Fig. 4.

A finite voltage drop is necessary for us to explain the appearance of strong, *stationary light-emission spots* at the tube-tube crossings. The reduced speed of the *ambipolar light-emission spot* as it goes through the loop crossings suggests that this is indeed the case. As long as the voltage drop across the loop crossing plus the kinetic energy of the carriers due to carrier heating effects [25] is of the order of a few hundred millivolts, carriers that elastically tunnel across the barrier at the crossings will have enough energy to excite electron-hole pairs which can radiatively recombine. If the voltage drop at a crossing would be larger than the nanotube bandgap of around 500mV, electrons could also tunnel from the valence band of one segment to the conduction band in the other.

The simple model is not able to produce different emission from n- and p- type conducting ideal CNTs, given the symmetry of the electron and holes in graphite. As we have indicated above however, the crossing of two carbon nanotubes strongly perturbs both tubes. There is substantial charge density in the contact region because of the proximity of the crossing tubes and the local deformation that they experience. [27] This can produce an asymmetry in the electron and hole barriers that strongly depends on the details of the particular crossing. The middle loop crossing in Fig. 4 is thus strongly active under p-type biasing conditions.

In addition to the loop-specific doping, there is however a reproducible trend in the relative intensity of the light emission from the different loop crossings: Whenever the *ambipolar spot* is positioned at one of the contacts, the nearby loop crossing shows enhanced luminescence. This is especially apparent at the top contact, which shows up exclusively in the n-type regime in Fig. 4B and in

the p-type regime in Fig. 4D. The more p-type character of the bottom contact prevents this one from showing up in the n-type regime in Fig. 4D when the *ambipolar spot* is in its vicinity. Nonetheless there is a big difference in intensity for this spot in the p-type regime. It shows up very strong in Fig. 4B where the *ambipolar spot* is close-by at the bottom contact, but its emission is absent when the *ambipolar region* is all the way at the opposite contact as in Fig. 4D. Tersoff et al. [4] have shown that a close-by *ambipolar spot* means that the charge density is low in the corresponding nanotube segment, while the electric field is high. (Current continuity requires that the product of charge density and carrier velocity is constant along the tube). Enhanced light emission at these crossings can thus be attributed to the higher field and a hotter carrier distribution at the crossing. Likewise, the extra intensity observed as the *moving spot* traverses the crossing is due to the hotter carrier distribution associated with the ambipolar region itself.

IV - CONCLUSION

The *stationary, localized electroluminescence* observed in this paper under unipolar conditions requires that electron-hole pairs be created at the locations along the carbon nanotube where the light emission is detected. This emission differs from the *moving spot emission* in ambipolar carbon nanotube FETs where the electron-hole pairs needed for radiative recombination across the CNT band-gap are naturally present when the electron and hole currents from the source and drain collide. *Stationary, localized electroluminescence* is of interest since it provides new information about how the electronic states of a carbon nanotube can be perturbed by the immediate environment. It also introduces a different method for the electrical excitation of light in carbon nanotubes other than through the ambipolar state which has been shown to be relatively inefficient and is limited to only one emission spot in a given FET.

We have identified two types of structural inhomogeneities in the environments of our carbon nanotube FETs which generate light emission. These are the boundaries of dielectric overlayers and the crossing of a looped nanotube. We also showed that other perturbations of the environment of a carbon nanotube FET can generate *localized, stationary light emission*. These include charge traps in the oxide and impurities on top of the device structure. Such inhomogeneities also produce observable changes in the electrical characteristics of the CNTFETs. The inhomogeneities are external to the body of a carbon nanotube. They generate spatially localized regions of high electric fields as well as discontinuities in the Fermi levels on either side of the inhomogeneities. The high fields produce energetic carriers. When combined with the discontinuities in the Fermi levels and the small bandgaps expected from our CVD generated carbon nanotubes, the hot carriers can create electron-hole pairs through impact ionization

processes which can radiatively recombine. The simultaneous measurement of light emission from naturally-occurring or introduced defects and of the associated current changes provides a powerful new approach for investigating the role of defects and environmental inhomogeneities in nanotube transport. One example discussed here involves the behavior of carriers at the crossings of carbon nanotubes. We find there can be significant transport of current across the tube crossing, and interesting differences between the behavior of ambipolar and unipolar currents at the crossings due to the role of electron-hole recombination.

Defect-related luminescence in unipolar carbon nanotubes provides enhanced electroluminescence efficiencies because the high-field conditions at the inhomogeneities establish an efficient route for minority carrier generation and multiplication. The strong current dependence of the light emission can be better exploited under unipolar biasing conditions where no *ambipolar light-emission spot* is present. Furthermore, the hot carrier distribution might mitigate the problem of low luminescence yields due to the presence of low-lying dark exciton states. Both dipole- and spin-forbidden (triplet) transitions have been predicted to lie below the lowest optically allowed excitation of nanotubes that could reduce the photo- and electro-luminescence yield. [31,32]. The demonstrated radiative recombination of hot carriers [2] and further reduction of the non-radiative relaxation rate as in suspended nanotubes may lead to a drastic yield enhancement of *localized electroluminescence*.

ACKNOWLEDGEMENTS

We thank V. Perebeinos and J. Tersoff for valuable discussions.

REFERENCES

[1] J. A. Misewich, R. Martel, Ph. Avouris, J. C. Tsang, S. Heinze, and J. Tersoff, Science **300**, 783 (2003).

[2] M. Freitag, V. Perebeinos, J. Chen, A. Stein, J. C. Tsang, J. A. Misewich, R. Martel, and Ph. Avouris, Nano Lett. **4**, 1063 (2004).

[3] M. Freitag, J. Chen, J. Tersoff, J. C. Tsang, Q. Fu, J. Liu, and Ph. Avouris, Phys. Rev. Lett. **93**, 076803 (2004).

[4] J. Tersoff, M. Freitag, J. C. Tsang, and Ph. Avouris, Appl. Phys. Lett. **86**, 263108 (2005).

[5] T. Ando, Semicond. Sci Technol. **15**, R13-27 (2000)

[6] C. T. White and T. N. Todorov, Nature **393**, 240-242 (1998).

[7] S.J. Tans and C. Dekker, Nature **404**, 834 (2000).

[8] M. Freitag, A. T. Johnson, S. V. Kalinin, and D. A. Bonnell, Phys. Rev. Lett. **89**, 216801 (2002).

[9] M. Freitag, M. Radosavljevic, W. Clauss, and A. T. Johnson, Phys. Rev. **B 62**, R2307 (2000).

[10] M. Ishigami, H. J. Choi, S. Aloni, S. G. Louie, M. L. Cohen, and A. Zettl, Phys. Rev. Lett. **93**, 196803 (2004).

[11] V. Perebeinos, J. Tersoff, and Ph. Avouris, Phys. Rev. Lett. **94**, 086802 (2005)

[12] S. Huang, X. Cai, and J. Liu, J. Am. Chem. Soc. **125**, 5636 (2003).

[13] W. Kim. A. Javey, O. Vermesh, Q. Wang, Y. Li, and H. Dai, Nano Lett. **3**, 193 (2003).

[14] J.R. Kirtley, M.B. Ketchen, K.G. Stawiasz, J.Z. Sun, W.J. Gallagher, S.H. Blanton, and S.J. Wind, Appl. Phys. Lett. **66**, 1138 (1995).

[15] M. S. Fuhrer, B. M. Kim, T. Dürkop, and T. Brintlinger, Nano Lett. **2**, 755 (2002).

[16] M. Radosavljevic, M. Freitag, K. V. Thadani, and A. T. Johnson, Nano Lett. **2**, 761 (2002).

[17] Below 15V, the device shows only the ambipolar light-emission spot with negligible hysteresis in the spot movement and the I-V_g characteristic. As V_d changes, the change in gate voltage at which the minimum in I_{sd} occurs is $\sim\Delta V_d/2$, as expected from conventional models of ambipolar behavior in CNTFETs. [M. Radosavljevic, S. Heinze, J. Tersoff, and Ph. Avouris, Appl. Phys. Lett. **83**, 2435 (2003).]

[18] Using the Schottky-barrier model for the conduction through the carbon nanotube and neglecting the voltage drop along the nanotube, we define two threshold voltages $V_{d,th}$ and $V_{s,th}$ at drain and source contacts that determine the onset of electron, or hole conduction. For gate voltages between these two values, $V_{d,th} < V_g < V_{s,th}$, the sub-threshold current decays exponentially as

$I \sim \left[\exp\left(V_{d,th} - V_g\right) + \exp\left(V_g - V_{s,th}\right) \right]$. A uniform trapped-charge profile ρ(x)=ρ along the carbon nanotube acts as an offset to both threshold voltages $V_{th,eff} = V_{th} + \alpha \cdot \rho$ and thus produces a shift in the gate-voltage characteristics that can explain our observed hysteresis. (The factor α depends on the relative strength of the nanotube - trapped charge coupling compared to the nanotube - backgate coupling and is thus a function of the distance between the traps and the carbon nanotube.) A non-uniform trapped-charge profile will affect one contact disproportionately, and the two threshold voltages will diverge. The minimum in conduction will then become much deeper in the presence of non-uniform charge trapping, as observed on the reverse sweep in Fig. 1C.

[19] M. Radosavljevic, S. Heinze, J. Tersoff, and Ph. Avouris, Appl. Phys. Lett. **83**, 2435 (2003).

[20] F. Liu, M. Bao, H. Kim, K. L. Wang, C. Li, X. Liu, and C. Zhou, Appl. Phys. Lett. **86**, 163102 (2005).

[21] S. M. Sze, Physics of Semiconductor Devices, (Wiley Interscience, New York 1969).

[22] J. Appenzeller, Y. M. Lin, J. Knoch, and Ph. Avouris, Phys. Rev. Lett. **93**, 196805 (2004).

[23] E. Nicollian and J. R. Brews, MOS Physics and Technology, (John Wiley and Sons, New York 1982).

[24] More rigorously, the effect of the charge density inside the carbon nanotube on the potential distribution along its length would have to be included in a self-consistent way, similar to the approach in ref [Ter05], but the simple picture already captures the essential feature of the slowing moving spot at the polymer boundary.

[25] C. D. Spataru, S. Ismail-Beigi, L. X. Benedict, and S. G. Louie, Phys. Rev. Lett. **92**, 077402 (2004).

[26] V. Perebeinos, J. Tersoff, and Ph. Avouris, Phys. Rev. Lett. **92**, 257402 (2004).

[27] M. S. Fuhrer, J. Nygard, L. Shih, M. Forero, Y.-G. Yoon, M. S. C. Mazzoni, H. J. Choi, J. Ihm, S. G. Louie, A. Zettl, and P. L. McEuen, Science **288**, 494 (2000).

[28] T. Hertel, R. E. Walkup, and P. Avouris, Phys. Rev. **B58**, 13870 (1998).

[29] S. Paulson, A. Helser, M. B. Nardelli, R. M. Taylor, H. M. R. Falvo, R Superfine, and S. Washburn, Science **290**, 1742 (2000).

[30] A. Buldum and J. P. Lu, Phys. Rev**. B63**, 161403 (2001).

[31] V. Perebeinos, J. Tersoff, and Ph. Avouris, arXiv:cond-mat/0506775 (2005).

[32] C. D. Spataru, S. Ismail-Beigi, R. B. Capaz, and S. G. Louie, arXiv:cond-mat/0507067 (2005).

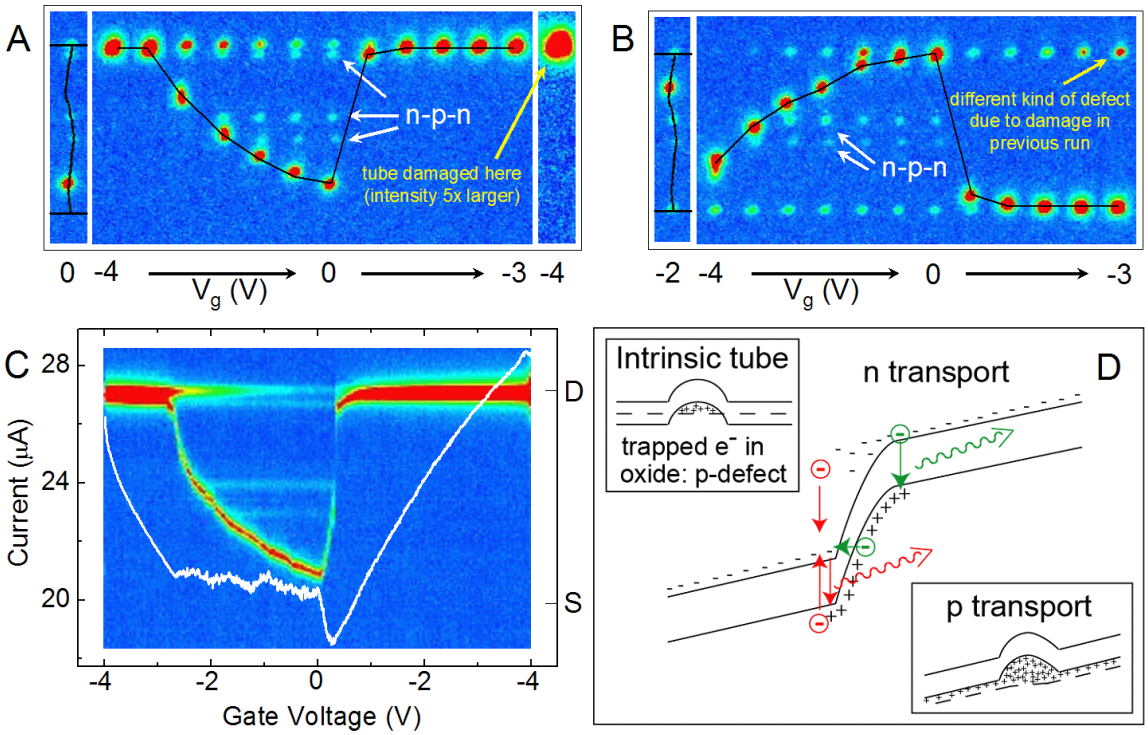

Figure 1. Light emission from intra-tube n-p-n junctions due to local p-type doping by oxide-trapped electrons. **(A)** Sequence of infrared images during a gate-voltage sweep (V_d=-30V). The carbon nanotube as imaged by SEM is shown in the first panel together with the luminescence at V_g=0V. The ambipolar spot, separating electron (above) and hole (below) conducting regions, is moving as illustrated by the solid black line. Additional spots are stationary and only appear for n-type conduction in the corresponding nanotube segment. **(B)** Sequence of infrared images with switched source and drain but otherwise identical voltages. The n-type region is now below and the p-type region above the ambipolar spot. The first panel shows the nanotube together with its electroluminescence at V_g=-2V on the forward sweep. **(C)** I-V_g characteristic (left axis) for the infrared sequence in (A). The projection of the luminescence onto a straight line connecting source and drain is shown on a false-color scale as a function of the applied gate voltage (right axis). **(D)** Proposed model for the stationary electroluminescence. A small nanotube segment is doped p-type by nearby trapped electrons in the gate oxide. For n-type conduction along the tube segment, an n-p-n junction produces luminescence. Two possible light-generation mechanisms are depicted in red and green. For p-type conduction no luminescence is observed.

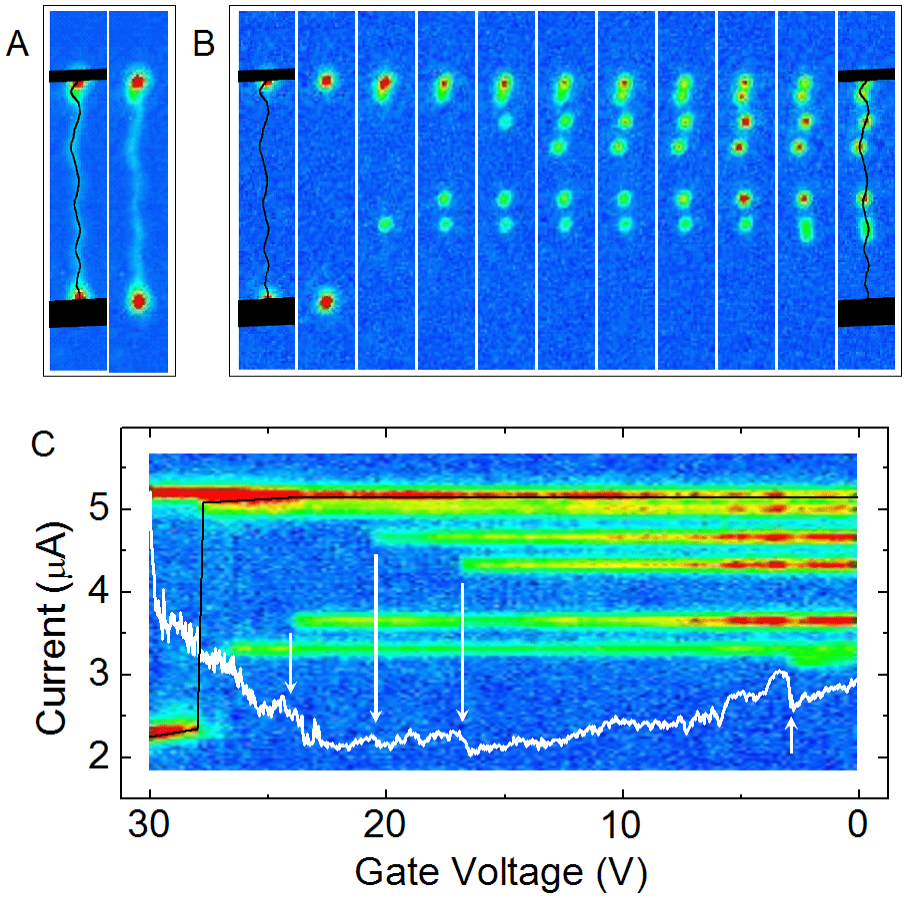

Figure 2. Correlation of electroluminescence and transport current from an un-protected carbon nanotube. **(A)** Light emission from the nanotube at 200C in a dry nitrogen atmosphere. The first panel shows an overlaid SEM image of the nanotube and its contacts. **(B)** Electroluminescence from the same carbon nanotube in air and at 200C during a gate-voltage sweep (V_g = 30V → 0V, V_d=40V). As the sequence progresses into a strong p-type regime, more and more stationary spots appear randomly. **(C)** Projection of the luminescence onto a straight line connecting source and drain contacts (false color) and gate-voltage characteristics. Each appearance of a new spot is accompanied by a drop in transport current. The solid line indicates the position of the ambipolar spot.

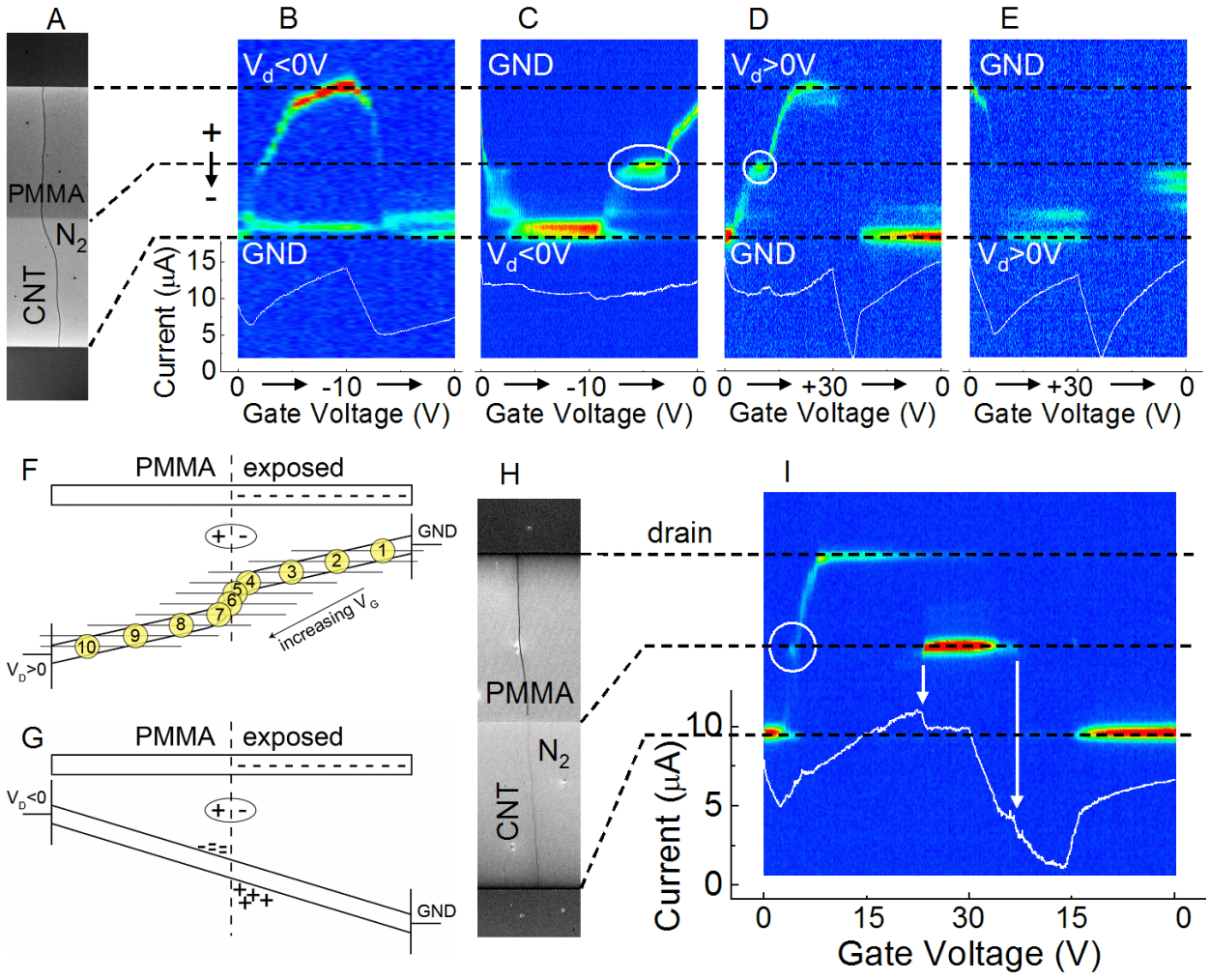

Figure 3. Effect of an environmental discontinuity (polymer boundary). **(A)** SEM image of a 50μm long CNTFET with a polymer layer covering the top half of the nanotube including its contact. **(B-E)** Projection of the infrared luminescence from this device onto an axis parallel to the carbon nanotube, and corresponding gate-voltage characteristic during which the luminescence was recorded. The drain voltage was -40V for (C) and (D) and +35V for (E) and (F). In (D) and (E), the ambipolar spot slows down as it passes-by the boundary because of the additional local voltage drop due to the dipole depicted between (B) and (C). **(F-G)** Schematic of the band bending in partially-PMMA-covered CNTFETs assuming electron trapping at the exposed side. The biasing conditions in (G) and (H) correspond to the situation in (E) and (C) respectively. **(H-I)** SEM image and luminescence/gate voltage characteristics for a different CNTFET. This device shows additional stationary luminescence at the polymer boundary during electron conduction accompanied by a sharp drop in both transport current and luminescence at the drain.

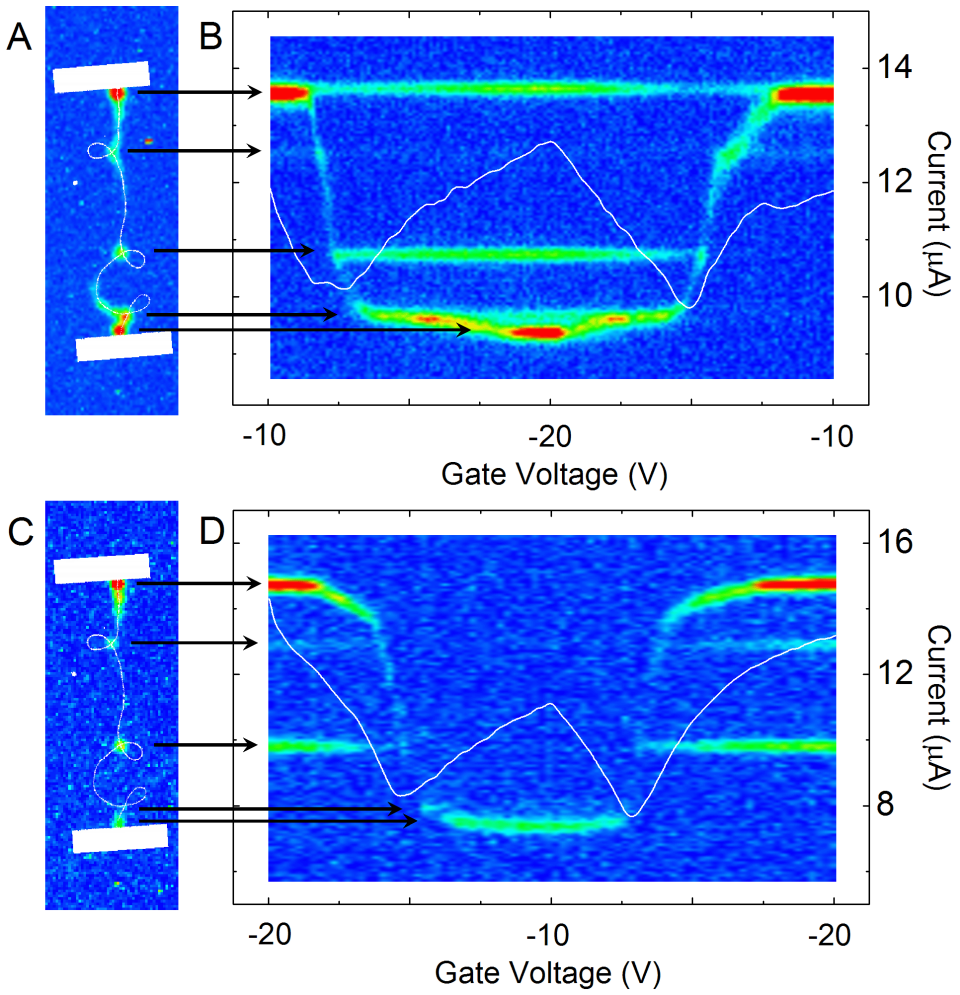

Figure 4. Electroluminescence from CNTFETs with loops. **(A)** Electroluminescence overlay image generated from the individual frames of an infrared video during a gate-voltage sweep. An SEM image of the carbon nanotube and its contacts is shown on top. **(B)** Projection of the luminescence onto a straight line connecting the top (source) and bottom (drain) contact (vertical axis) as a function of the time during the gate-voltage sweep (horizontal axis). (V_d=-40V, V_g= -10V → -20V → -10V). **(C-D)** same as (A-B), but different biasing conditions: Source and drain switched, V_d=-35V, and V_g= -20V → -10V → -20V.

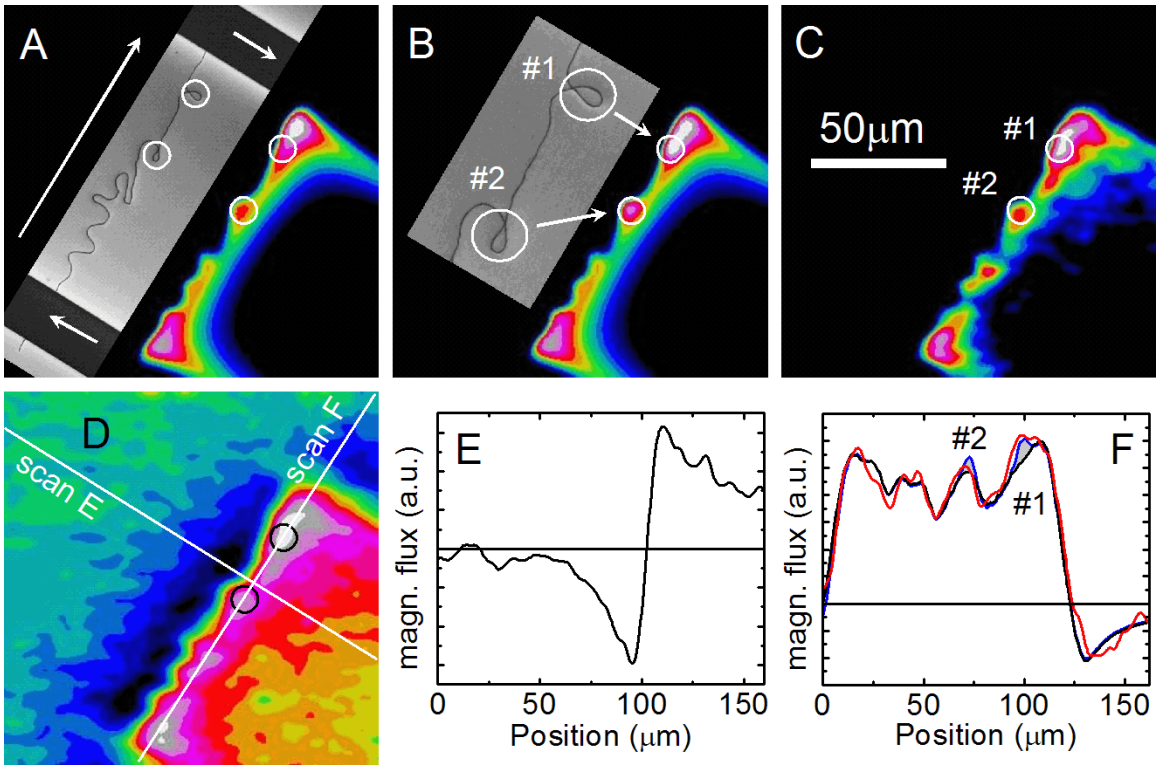

Figure 5. Scanning SQUID microscopy of nanotube loops. **(A)** Modeled SQUID image under the assumption of 100% current tunneling through the nanotube-nanotube junctions. **(B)** Modeled SQUID image under the assumption of 100% current flowing through the loops. **(C, D)** Experimental SQUID image from the CNTFET shown in two different color scales. In (C) the color scale is similar to the one in the two models; In (D) the full data scale is shown. **(E)** Trace perpendicular to the carbon nanotube at the position indicated in (D). **(F)** Trace parallel to the carbon nanotube, intersecting both loops as shown in (D). The blue and black curves correspond to the modeled data with and without current through the loops. The difference between the two models is shaded in gray. The red curve represents the experiment.